Empirical correspondence between trophic transfer efficiency in freshwater food webs and the slope of their size spectra

Thomas Mehner https://orcid.org/0000-0002-3619-165X, Kristin Scharnweber https://orcid.org/0000-0003-2858-5947, Katrin Attermeyer https://orcid.org/0000-0002-6503-9497, Ursula Gaedke https://orcid.org/0000-0003-2900-6847, Sabine Hilt https://orcid.org/0000-0002-0585-2822 and Sandra Brucet https://orcid.org/0000-0002-0494-1161

DOI
doi:10.1002/ecy.2347

Original publication date
1 June 2018 (Version of record online)

Document version
Accepted version

Published in
Ecology

Citation
Mehner T, Lischke B, Scharnweber K, Attermeyer K, Brothers S, Gaedke U, Hilt S, Brucet S. Empirical correspondence between trophic transfer efficiency in freshwater food webs and the slope of their size spectra. Ecology. 2018;99(6):1463-72.

Empirical correspondence between trophic transfer efficiency in freshwater food webs and the slope of their size spectra

Thomas Mehner[1,*], Betty Lischke[1], Kristin Scharnweber[1,2], Katrin Attermeyer[1,2], Soren Brothers[1,3], Ursula Gaedke[4], Sabine Hilt[1], Sandra Brucet[5,6]

[1] Leibniz-Institute of Freshwater Ecology and Inland Fisheries, Müggelseedamm 301 & 310, 12587 Berlin, Germany

[2] Department of Ecology and Genetics, Limnology; Uppsala University, Norbyvägen 18D; 75236, Uppsala, Sweden

[3] Department of Watershed Sciences and Ecology Center, Utah State University, 5210 Old Main Hill, Logan, Utah, 84322-5200, USA

[4] Institute for Biochemistry and Biology, University of Potsdam, Potsdam, Germany

[5] University of Vic - Central University of Catalonia, Aquatic Ecology Group, Vic, Catalonia, Spain

[6] Catalan Institution for Research and Advanced Studies ICREA, 08010 Barcelona, Catalonia, Spain

[*]Correspondence to: mehner@igb-berlin.de

Running head: Size spectra and transfer efficiency

Abstract

The density of organisms declines with size, because larger organisms need more energy than smaller ones and energetic losses occur when larger organisms feed on smaller ones. A potential expression of density-size distributions are Normalized Biomass Size Spectra (NBSS), which plot the logarithm of biomass independent of taxonomy within bins of logarithmic organismal size, divided by the bin width. Theoretically, the NBSS slope of multi-trophic communities is exactly -1.0 if the trophic transfer efficiency (TTE, ratio of production rates between adjacent trophic levels) is 10% and the predator-prey mass ratio (PPMR) is fixed at 10^4. Here we provide evidence from four multi-trophic lake food webs that empirically estimated TTEs correspond to empirically estimated slopes of the respective community NBSS. Each of the NBSS considered pelagic and benthic organisms spanning size ranges from bacteria to fish, all sampled over three seasons in one year. The four NBSS slopes were significantly steeper than -1.0 (range -1.14 to -1.19, with 95% CIs excluding -1). The corresponding average TTEs were substantially lower than 10% in each of the four food webs (range 1.0% to 3.6%, mean 1.85%). The overall slope merging all biomass-size data pairs from the four systems (-1.17) was almost identical to the slope predicted from the arithmetic mean TTE of the four food webs (-1.18) assuming a constant PPMR of10^4. Accordingly, our empirical data confirm the theoretically predicted quantitative relationship between TTE and the slope of the biomass-size distribution. Furthermore, we show that benthic and pelagic organisms can be merged into a community NBSS, but future studies have yet to explore potential differences in habitat-specific TTEs and PPMRs. We suggest that community NBSS may provide valuable information on the structure of food webs and their energetic pathways, and can result in improved accuracy of TTE-estimates.

Key words: Normalized biomass size spectra, trophic transfer efficiency, pelagic and benthic lake habitats, size of organisms, energetic equivalence rule, multi-trophic communities

Introduction

The relationship between body size, density, and energy use of organisms is a central research topic in ecology (White et al. 2007). The often observed exponential decline of densities (D) of populations sharing a common resource with average body size (M) at $D \sim M^{-0.75}$ (Damuth 1981, Nee et al. 1991) is caused by energy availability, which directly modifies the density of organisms, mediated by the size-dependent metabolic rates of the individuals (Metabolic Theory of Ecology, MTE, Brown et al. 2004). However, the exponent of empirical density-size distributions of all organisms independent of taxonomy at a certain location is often substantially smaller than -0.75 (Gaedke 1992, Cyr 1997, Marquet 2000). In these communities forming multi-trophic food webs in which larger organisms feed on smaller ones, energy is lost by trophic transfer between trophic levels. Accordingly, the total energy available to larger organisms is lower than that for smaller organisms, resulting in more negative exponents of density-size distributions than predicted (as above) for populations where all individuals use the same resource.

The energy transfer within multi-trophic food webs is quantified by the trophic transfer efficiency (TTE), which is the proportion of resource (prey) production converted into consumer (predator) production. It has traditionally been assumed that the TTE between adjacent trophic levels is roughly 10% (Lindeman 1942). The size relationships between predator and prey are quantified by the predator-prey mass ratio (PPMR), which is assumed to be around 10^4 in aquatic open-water habitats (Trebilco et al. 2013). Therefore, the exponent of the density-size distribution is theoretically predicted to decline from -0.75, when all organisms feed on the same resource, to exactly -1.0 in multi-trophic food webs with TTE=10% and PPMR=10^4 (see Theoretical Background below). This TTE-correction of the density-size distributions combines two independently developed relationships, the decline of density with size (summarized by Brown et al. 2004), and the concept of trophic levels connected by predator-prey interactions, in which only a part of the total energy is transferred

from one level to the next (summarized by Trebilco et al. 2013). Both concepts are based on independent empirical observations, yet they share the common physiological basis that the density of organisms is dictated by the size-dependent balance between available resources and metabolic efficiency.

The trophic level concept of predators being less abundant and larger than their prey is supported by studies of the open-water areas of aquatic ecosystems. Accordingly, exponents <-0.75 of density-size distributions were often found in multi-trophic food webs in these habitats (Brown and Gillooly 2003, Reuman et al. 2008). Furthermore, an earlier study in Lake Constance (Germany/Switzerland/Austria) has shown corresponding changes in PPMR, TTE, and exponents of density-size distributions across several samplings within a single year (Gaedke et al. 1996). However, we intended to expand the empirical confirmation of the TTE-correction by demonstrating the quantitative correspondence between the exponents of density-size distributions for multi-trophic food webs and their transfer efficiencies across multiple ecosystems. Hence, we adopted a community energy perspective and focused on the interplay between TTE and the NBSS slope by assuming a fixed PPMR, although mechanistic explanations may also be provided by process-based models which considered individual predator-prey interactions resulting in similar energetic constraints (e.g., Kerr and Dickie 2001, Andersen and Beyer 2006, Law et al. 2009, Hartvig et al. 2011, Rossberg 2012).

Community size distributions composed of several trophic levels are often expressed as abundance or biomass size spectra, especially in aquatic systems (Sprules and Barth 2016). Size spectra are linear regressions between the logarithm of either abundance or biomass *vs*. the logarithm of body mass, as obtained by logarithmic binning. The slopes of these linear log-log regressions are related to the exponent of the density-size distributions. If the size spectra are normalized by the width of the respective size class, the slope of the normalized biomass size spectrum (NBSS) can be used to directly estimate the exponent of the biomass-size distribution (White et al. 2008). Most of the aquatic community size spectra published so

100 far for lakes only included phytoplankton, zooplankton, and occasionally fish (Sprules 2008,
101 Yurista et al. 2014). In rare cases, protozoa and bacteria have also been included (Gaedke
102 1992, Gaedke et al. 1996). Surprisingly few studies have incorporated the benthic habitats of
103 lakes, although size spectra are available for marine benthic communities (Blanchard et al.
104 2009, Rogers et al. 2014). Benthic and pelagic (water column) food chains may be closely
105 linked (Vadeboncoeur et al. 2002, Brothers et al. 2016), but the integration of benthic and
106 pelagic size spectra into a single community biomass spectrum has never been conducted in
107 freshwater ecosystems.

108 In this study, we aimed to demonstrate that the TTE and the slope of a community NBSS
109 are quantitatively related, thus empirically confirming the hypothesized TTE-correction of the
110 biomass-size distributions. We measured the biomass and size of benthic and pelagic
111 organisms ranging from bacteria to fish in four separate lake food webs, and calculated
112 biomass spectra slopes. Furthermore, we measured the TTE in each of the four food webs by
113 comparing primary and bacterial production with consumer secondary production, and
114 predicted the respective slopes of biomass spectra according to the TTE-correction. Finally,
115 by integrating benthic and pelagic food webs into the same NBSS, we explored differences in
116 biomasses of producer and consumer groups between these habitats through examining the
117 systematic residual variations of these groups from the slopes of the community size
118 distributions.

119

120 **Methods**

121 *Theoretical background*

122 Following Reuman et al. (2008), the size distribution of individuals sharing a common
123 resource is a power law of individual size (*M,* mass) in the form of

124 $$f(M) \propto M^{-1.75} \quad (1)$$

In communities where organisms from the lowest trophic level are the only ones to exploit the basal resource, and larger organisms from higher trophic levels consume smaller organisms from lower trophic levels, a decrease of abundance with increasing size is also influenced by the energy transfer efficiency between trophic levels and the size relationships between predator and prey. Accordingly, the community abundance distribution can be estimated as

$$f(M) \propto M^{\frac{\log(TTE)}{\log(PPMR)}-1.75} \quad (2)$$

With TTE = trophic transfer efficiency between trophic levels and PPMR = average predator-prey body mass ratio, assuming neither TTE nor PPMR vary systematically with *M*. This assumption is appropriate for the predator-prey pairs typically dominating open-water habitats of aquatic ecosystems. Because biomass (*B*) is the product of numbers (*N*) and *M*, the community biomass distribution is

$$f(B) \propto M^{\frac{\log(TTE)}{\log(PPMR)}-0.75} = M^{\alpha} \quad (3)$$

with α being the exponent of the power law of *B* with *M*. By considering a PPMR of 10^4 (10,000) and a TTE of 10% (10^{-1}) (Pauly and Christensen 1995, Trebilco et al. 2013),

$$\alpha = \frac{\log(0.1)}{\log(10{,}000)} - 0.75 = -1 \quad (4)$$

The slope β of the linear regression between log biomass and log body size in logarithmic bins (biomass size spectrum, BSS) is zero. Therefore, the exponent α can be indirectly estimated as

$$\alpha = \beta - 1 \quad (5)$$

However, normalizing the BSS by the width of the respective size class (normalized biomass size spectrum, NBSS) reduces the slope by 1, and hence the NBSS slope can be used to directly estimate α (White et al. 2008). For communities with TTE=10% and PPMR=10^4, α=-1. For communities with TTE<10% and PPMR=10^4, the TTE-correction predicts α<-1 and β<0. These predictions are equivalent to a TTE-corrected Energetic Equivalence Rule (ERR),

150 as proposed earlier (Damuth 1981, Nee et al. 1991). The EER emerges from the size-
151 dependency of metabolic rates of organisms (exponent=0.75) combined with an exponential
152 decline of population densities sharing a common resource with average body size
153 (exponent=-0.75), resulting in a power law stating that energy use scales with organismal size
154 with an exponent of zero. The EER likewise predicts that the energy-use scaling in multi-
155 trophic food webs would decline from zero to -0.25 through TTE and PPMR corrections
156 (Reuman et al. 2008, Trebilco et al. 2013).
157
158 *Empirical background*
159 Data were obtained from whole-lake experiments conducted in two lakes, Schulzensee and
160 Kleiner Gollinsee (hereafter referred to as Gollinsee), both located in northeastern Germany.
161 Both lakes were eutrophic (32-40 µg total phosphorus L^{-1}), shallow (mean depth about 2 m)
162 and small (3-4 ha surface area), but only Schulzensee contained submerged macrophytes
163 (Brothers et al. 2013). We conducted whole-lake experiments as part of an unrelated project
164 starting in October 2010 (Scharnweber et al. 2014, Mehner et al. 2016), for which both lakes
165 were divided in an east-west direction by a plastic curtain, producing fully isolated, equally
166 sized halves. These long-term lake divisions created lake halves with some differences in the
167 dominant organism groups. Consequently, we consider the north and south halves of both
168 lakes as independent replicates for subsequent calculations (see results for confirmation of
169 this assumption).
170
171 *Sampling*
172 Sampling was conducted in spring (April), summer (June), and autumn (October) 2011.
173 Organism biomasses were converted to g carbon (C) per m^2 and individual mass was
174 converted to g C (see Appendix S1 for details of conversions between units). Bacteria,
175 phytoplankton, and zooplankton measurements from pelagic and littoral locations were

176 arithmetically averaged as we assumed the lake waters to be horizontally well mixed, as
177 indicated by similar planktonic community compositions and biomasses at both locations. We
178 refer to these samples as pelagic, in contrast to samples from the benthic habitats (sediment
179 bacteria and benthic macroinvertebrates). Sampling details have been described elsewhere
180 (Brothers et al. 2013, Mehner et al. 2016), and the procedures are summarized in Appendix
181 S1. Biomasses and sizes were measured for pelagic and benthic bacteria, 65 phytoplankton
182 morphotypes, 39 ciliate morphotypes, 37 rotifer morphotypes, 47 crustacean morphotypes, 15
183 macrozoobenthos morphotypes, and individual sizes of 5 fish species (Appendix S1, Table
184 S1).
185
186 *Biomass size spectra*
187 To calculate size spectra, we allocated the biomass of all organisms (from bacteria to fish)
188 into logarithmically-binned body size classes (biomass size spectrum, BSS, expressed in C
189 units). Therefore, the average C mass per organismal morphotype (bacteria, phytoplankton,
190 ciliates, rotifers, crustaceans, macrozoobenthos) or individual mass (fish) was assigned to one
191 of fifty-three $\log_2$ size classes (1st class $>2^{-45.5}$~20 fg C ind^{-1} to $\leq 2^{-44.5}$~40 fg C ind^{-1}; … 53rd
192 class $>2^{6.5}$~90 g C ind^{-1} to $2^{7.5}$~180 g C ind^{-1}; Appendix S1, Table S1, Figure S1), and the
193 respective biomasses of morphotypes were summed per size class. Morphotypes partly
194 overlapped in size such that occasionally different groups of organisms were pooled within a
195 single $\log_2$ size class. To account for size variability within bacterial groups resulting, for
196 instance, from cell division, the measured bacterial biomass was distributed over three $\log_2$
197 size classes by assigning only 50% of the biomass to the average size class of the respective
198 bacterial group and allocating 25% each to the neighboring lower and higher size classes. This
199 biomass distribution roughly corresponded to the size distribution obtained from single- cell
200 measurements during some of the sampling days (B. Lischke, unpubl. results).

The biomass per $\log_2$ size class was divided by the width of the respective size class to normalize the size spectrum (normalized biomass size spectrum, NBSS, White et al. 2008). The normalized biomass is numerically close to the abundance per size class. The slope of the NBSS was obtained from linear least-squares regressions between the logarithm of the normalized summed biomass per $\log_2$ size class and the midpoint of each $\log_2$ size class. The NBSS slope is identical to the exponent of the TTE-corrected biomass-size distribution (α) (White et al. 2008), and hence at TTE=10% and PPMR=10^4, the theoretical NBSS slope would be -1. We calculated three size spectra per lake half (one from each sampling season), resulting in twelve spectra in total, incorporating all organisms from bacteria to macrozoobenthos. Fish data were available only in autumn, and hence we created one additional size spectrum per lake half, which included fish.

Applying linear regression models to size data binned in linear or logarithmic size classes results in a loss of the biomass variability over the size gradient within a binned size class, which may lead to inaccurate estimates of the NBSS slope. This can be circumvented using continuous size distributions (White et al. 2008). However, exact sizing of all individual organisms from bacteria to fish was impossible because of the numerous morphotypes included in each trophic group. We instead had to rely on the average size and biomasses of morphotypes in many groups of organisms, and there was thus no alternative except to calculate the NBSS slope by linear regression.

Trophic transfer efficiency

In a recent study, we assessed the biomass and production of autotrophs, bacteria, and consumers in the pelagic and benthic habitats of the northern halves of Gollinsee and Schulzensee and aggregated these data to seasonally-averaged quantitative food webs (Lischke et al. 2017). Subsequently, trophic transfer efficiencies (TTEs) were calculated as the ratio of consumer production to resource production, hence indicating the efficiency of

227 resource utilization by the consumers. To obtain similar estimates for the southern halves of
228 both lakes, quantitative food webs and TTE calculations were repeated following the same
229 approach. In short, we calculated the gross and net primary production (GPP, NPP) of
230 submerged macrophytes from summer biomass measurements (Best 1982). The GPP of
231 phytoplankton was calculated every two to four weeks from the measured quantum yield of
232 photosystem II, specific absorption cross section, the efficiency of carbon assimilation, and
233 the intensity of photosynthetically active radiation at 10 cm depth intervals (Brothers et al.
234 2013). For periphyton (epiphyton and epipelon), submerged plastic strips were exposed in the
235 pelagic zone at 1.2 m below the surface to measure monthly periphyton biomass accumulation
236 and production rates, which were then converted to epiphyton and epipelon production based
237 on measurements of underwater plant surface area and sediment surface area estimates,
238 respectively (Brothers et al. 2013). Algal NPP rates were estimated from measured GPP rates
239 (details provided in Lischke et al. 2017). Bacterial production rates were measured via the
240 incorporation of L-^{14}C leucine into the protein fraction (following Simon and Azam 1989 for
241 water, and Buesing and Gessner 2003 for sediments). Rotifer production rates were estimated
242 using a linear regression model accounting for total biomass and temperature (Shuter and Ing
243 1997). Production estimates for crustaceans were based on the individual size and biomass of
244 each species using two sets of specific parameters for water temperatures above and below
245 10°C (Stockwell and Johannson 1997). The annual macrozoobenthos production was
246 estimated using the allometry-based approach of Plante and Downing (1989), which includes
247 macrozoobenthos biomass, individual mass, and ambient temperature. For each of the four
248 lake halves, we calculated the TTE as the ratio between the sum of macrozoobenthos, rotifer,
249 and crustacean production, divided by the sum of bacterial (sediment and pelagic) and
250 autotrophic (phytoplankton, periphyton, epipelon, and macrophyte) production. These four
251 groups of primary producers contributed to the diet of the consumers in both lakes (Syväranta
252 et al. 2016).

Analyses

To evaluate whether the empirically determined NBSS slope deviated from -1, we checked whether the 95% confidence intervals (CIs) of the slopes excluded -1. For a more detailed analysis, we calculated a linear mixed effect model (LMM). The model included lake, sampling season, lake division (north vs. south), the interaction of lake with size class, and the interaction of lake division with size class all as fixed effects, and further accounted for the serial autocorrelation within lake halves by including a random effect as:

$\log_2$(normalized biomass) ~ $\log_2$ size class + lake + season + lake division + lake : $\log_2$ size class + lake division : $\log_2$ size class + (1|lake half). (5)

This LMM was defined to test for differences in the slopes of the NBSS between the four lake halves, excluding fish. Hence, we considered only the full model and did not perform model selection. A non-significant lake-division effect would justify our approach to consider both lake halves as replicates. A significant lake-by-size-class interaction would indicate different NBSS slopes between the lakes and a significant lake-division-by-size-class interaction would indicate different NBSS slopes between northern and southern lake halves.

To evaluate whether the biomasses of certain producer or consumer groups deviated systematically from the slope of the NBSS, we merged all available biomass-size data pairs (n=1122) from all lake halves and calculated an average slope for all measurements by linear least-squares regression. We then calculated the arithmetic average residuals from the regression for each organismal group to assess group-specific deviations from the community-wide biomass-size relationship. In cases where more than one organismal group contributed to the biomass of a single size class (13 out of 38 size classes excluding fish), the biomass of the size class was assigned to whichever organismal group dominated by biomass.

The empirically estimated NBSS slopes in the four lake halves were correlated with the theoretical NBSS slopes as predicted from the lake-half specific TTE (equation 3, assuming a constant PPMR=10^4) by Spearman's rank correlation coefficient. The arithmetic average of

empirical TTEs from the four lake halves was compared with the slope of the aggregated NBSS of the four lake halves.

Statistical analyses were performed in R version 3.2.4 (R Core Team 2016) using the packages lme4, lmerTest and lsmeans for the linear mixed effect model analyses.

Results

The community-wide NBSS from bacteria to fish covered 53 $\log_2$ size classes. The NBSS slopes from bacteria to macrozoobenthos of each lake half per season ranged from -1.21 to -1.13 (Fig. 1). The 95% confidence intervals of all slopes overlapped, and did not include -1 (Fig. 1). When fish size-biomass data were included, the slopes became slightly less steep than those covering only bacteria to macrozoobenthos, ranging from -1.15 to -1.08, with their CIs likewise excluding -1 (Appendix S1, Figure S2). However, the CIs overlapped with those of the NBSS without fish.

Merging all biomass-size measurements from bacteria to macrozoobenthos across the three sampled seasons, but separately for all four lake halves, provided an average slope of -1.14 [95% CI :-1.2, -1.09] for Gollinsee (north), -1.19 [-1.24, -1.13] for Gollinsee (south), -1.17 [-1.22, -1.12] for Schulzensee (north) and likewise -1.17 [-1.22, -1.11] for Schulzensee (south). These slopes did not differ between the four lake halves (Table 1, linear mixed model; non-significant interactions lake-by-size class and lake division-by-size class, Appendix S1, Table S2).

The overall slope of the NBSS, merging all data from bacteria to macrozoobenthos from both northern and southern halves of both lakes in each season, was -1.17 [-1.19, -1.14] (Fig. 2). The average group-wise residuals from this regression line were positive for sediment bacteria, ciliates, and macrozoobenthos, whereas pelagic bacteria, rotifers, and crustaceans had negative residuals (Table 2).

Whole-lake TTEs, comparing the sum of rotifer, crustacean, and macrozoobenthos production (primary consumers) against the sum of pelagic and benthic autotrophic and bacterial production, were 3.5% and 1.5% in northern and southern halves of Schulzensee, respectively, and 1.4% and 1.0% in northern and southern halves of Gollinsee, respectively (Appendix S1, Figure S3). By assuming a PPMR of 10^4, these TTEs result in NBSS slopes ranging between -1.25 (Gollinsee, south), -1.21 (Gollinsee, north and Schulzensee, south), and -1.11 (Schulzensee, north).

There was no correlation between the empirically determined slopes in the four lake halves and the slopes predicted from the empirically estimated TTEs (Spearman's rho=0.22, P=0.68, Fig. 3). However, the overall slope merging all biomass-size data pairs from the four lake halves (-1.17) was almost identical to the slope (-1.18) predicted from the arithmetic mean TTE (1.85%) from the four lake halves (Fig. 3).

Discussion

Our analyses indicated that the slopes of the community NBSS from bacteria to macrozoobenthos in both lakes and in their northern and southern halves were always significantly more negative than -1, suggesting that the TTE in these four food webs was substantially lower than 10%. Empirical estimates in the lakes confirmed that the TTE between producers and primary consumers ranged from 1% to 3.5%. The differences in TTE between the four lake halves did not correlate with the NBSS slopes in the respective food webs. However, if the average TTE from all four food webs was used to predict the slope of the combined NBSS from all four lake halves, predicted and empirically estimated average slopes matched very closely. Accordingly, our empirical results from aquatic ecosystems confirm the theoretically predicted relationship between TTE, PPMR and NBSS slope (Brown and Gillooly 2003, Reuman et al. 2008, Trebilco et al. 2013).

330 *Variables affecting the biomass-size distributions*

331 All 12 NBSS slopes covering bacteria to macrozoobenthos and the four slopes additionally
332 including fish were significantly steeper than -1. The significant deviations from -1 support
333 the proposed relationship between the efficiency of energy transfer in food webs and the
334 biomass-size distribution of the respective organisms (Brown et al. 2004, Trebilco et al.
335 2013). By considering the estimated TTE between 1% and 3.5% in the four lake halves, a
336 size-related allometric metabolism exponent of 0.75 and a uniform PPMR of 10^4, the expected
337 NBSS slopes ranged between -1.25 and -1.11 (Appendix S1, Table S3). This range coincided
338 with the range of the NBSS slopes measured in both lakes (-1.14 to -1.19). However, the rank
339 of measured TTE in the four lake halves did not correspond with the rank of the slopes in the
340 four lake halves, and the CIs of the slopes overlapped between all four lake halves. This
341 mismatch in rank order between NBSS slopes and empirically determined TTE suggests that,
342 among other things, the precision of biomass, size, and production measurements was not
343 high enough to generate statistically detectable differences between lake halves. However, a
344 significant deviation from the expected NBSS slope of -1 has been documented in our
345 empirical data, which confirms that the efficiency of energy transfer within food webs is
346 reflected by the slopes of community-wide NBSS.

347 The second variable in the biomass-size distribution model is the PPMR, which has been
348 fixed at 10^4 for our calculations, following earlier suggestions (Brown and Gillooly 2003,
349 Trebilco et al. 2013). However, less is known about the true PPMR in aquatic food webs.
350 Estimating the average PPMR in the four lake halves would have required detailed stomach
351 and gut content or stable isotope analyses for all individual consumers (Jennings et al. 2002),
352 an effort we could not accomplish because of the large number of differing morphotypes and
353 species characterized in the food webs of both lakes (Appendix S1, Table S1). However, the
354 range of potential PPMRs as based on the size ranges of all broadly defined invertebrate

355 predator-prey pairs such as ciliates-pelagic bacteria, ciliates-phytoplankton, rotifers-
356 phytoplankton and crustaceans-phytoplankton includes 10^4 (Appendix S1, Table S1).
357 Generally, the variation in the NBSS slope caused by variation in PPMR is relatively
358 small. A hypothetical reduction or increase of the PPMR to 10^3 or 10^5 causes an NBSS slope
359 of -1.08 and -0.95, respectively, assuming a fixed TTE at 10%. Therefore, with a TTE of
360 10%, the global NBSS slope calculated across all four lake halves (-1.17) would predict a
361 PPMR as low as 240 (Appendix S1, Table S3), almost two orders of magnitude lower than the
362 commonly assumed PPMR of 10^4. Empirical estimates support that ciliates have a PPMR of
363 about 10^3, rotifers, nauplii, and copepodites have a PPMR of 10^4, and PPMRs even greater
364 than 10^4 were found for cladocerans and meroplankton (Hansen et al. 1994). A PPMR of 10^6
365 has been empirically determined for invertebrate and fish communities in the central North
366 Sea (Jennings and Mackinson 2003). Consequently, an average PPMR of 10^4 across all
367 feeding levels in our lakes seems reasonable and indicates that the low NBSS slopes have
368 been caused primarily by the low TTE. Overall, a TTE in the range of 1% to 3%, as observed
369 in our lakes, would always result in NBSS slopes <-1.1 for every PPMR in the range of 10^0 to
370 10^4 (Trebilco et al. 2013).
371 The metabolic theory of ecology predicts that the metabolic rate (MR) of organisms scales
372 with body mass (M) as $MR \sim M^{0.75}$ (Brown et al. 2004). The true values of the allometric
373 exponent and potential variations between organismal groups are under debate. For example,
374 Lake Constance phyto- and zooplankton exhibited an allometric exponent of 0.85 (De Castro
375 and Gaedke 2008), which would produce a slope of -1.1 at a TTE of 10%, and a PPMR of 10^4
376 (Appendix S1, Table S3). In turn, the empirically measured average NBSS slope of -1.17
377 across all four lake halves, combined with an allometric exponent of 0.85 and PPMR of 10^4
378 would result in an average TTE of 5.2%, which is outside the range of the estimated TTEs in
379 Gollinsee and Schulzensee. Therefore, a metabolic exponent for all involved organisms
380 substantially larger than 0.75 would have produced NBSS slopes substantially more negative

381 than -1, even without low TTEs. However, there are no systematic studies on the metabolic
382 exponents of entire aquatic communities, and hence it is reasonable to apply 0.75 as the
383 average metabolic coefficient (Brown et al. 2004).
384
385 *Community-wide size spectra*
386 We generated community-wide size spectra, which included organisms from bacteria to
387 fish ranging over 53 $\log_2$ size classes. This range is equivalent to 17 $\log_{10}$ size classes, and
388 hence among the widest size ranges for aquatic size spectra reported in the scientific literature
389 (Sheldon et al. 1972, Gaedke 1992, Sprules 2008, Yurista et al. 2014). Furthermore, we
390 derived community size spectra by combining pelagic and benthic organisms, which are often
391 considered to form spatially separate food webs (Vadeboncoeur et al. 2002). However, the
392 benthic habitat was represented only by bacteria and macrozoobenthos in our study. The
393 integration of benthic organisms into community size spectra is still in its infancy (Blanchard
394 et al. 2009, Rogers et al. 2014, Blanchard et al. 2017). If benthic autotrophs such as epiphytes
395 and epipelon have roughly the same size distribution as pelagic autotrophs, their biomasses
396 would add to the biomasses per size group now covered by phytoplankton alone, and this may
397 have an effect on the NBSS slope. However, a strong leverage effect from biomass variability
398 of size groups in the middle of the distribution (such as phytoplankton or epiphyton) is highly
399 unlikely, and hence the omission of benthic autotrophs from the NBSS should have only a
400 marginal effect on the overall slope. Furthermore, we were unable to sample meiobenthic
401 organisms properly. The few studies on freshwater meiobenthos size structure (Morin and
402 Nadon 1991) suggest that most of the meiobenthos biomass is in the size classes larger than 2
403 mm (about 5 μg C per individual), which corresponds to a conspicuous trough in our size-
404 frequency distributions (Appendix S1, Figure S1). Accordingly, it is likely that biomass-size
405 data pairs of meiobenthos would fit into this trough without modifying the NBSS slope
406 substantially. By including only macrozoobenthos and sediment bacteria, we could not

407 calculate a separate NBSS for benthic habitats. However, future empirical comparisons of
408 slopes and intercepts between pelagic and benthic size spectra for the same locality may
409 reveal insights into potentially systematically differing TTE and PPMR between habitats
410 (Blanchard et al. 2017).

411 Previous detailed analyses of the feeding interactions in the pelagic habitat of both lakes
412 have shown that crustacean biomasses were reduced and ciliate biomasses increased as a
413 consequence of a partial winter fish kill (Hilt et al. 2015, Lischke et al. 2016). The resulting
414 strong predation pressure by ciliates likely reduced the biomass of small phytoplankton and
415 pelagic bacteria and benefitted large phytoplankton species (Lischke et al. 2016).
416 Furthermore, quantitative analyses of C fluxes within Gollinsee and Schulzensee have
417 indicated that the production of sediment bacteria was only partly converted into consumer
418 production, resulting in high biomasses of benthic bacteria (Lischke et al. 2017). The average
419 residuals for each organismal group from the global NBSS slope calculated in this study
420 reflected these deviations, as we found strongly negative residuals for pelagic bacteria and
421 crustaceans, and strongly positive residuals for sediment bacteria, ciliates, and the larger
422 phytoplankton morphotypes. Surprisingly, the global NBSS slope, which reflects the TTE of
423 the entire food web, is relatively insensitive to these substantial deviations of organismal
424 biomass from the biomass predicted according to the TTE-corrected biomass-size
425 distributions (Sprules 2008). Overall, such an invariance of community NBSS slopes, despite
426 biomass variations of single organismal groups in the dimension of one or two magnitudes,
427 suggests that a strong depletion of biomass in single prey groups by predators may be
428 balanced by compensatory increases in the biomass of less-utilized prey groups. From that
429 perspective, the community NBSS slope poorly reflects the biomass pools in food webs,
430 which result from the varying intensity of several trophic interactions.

431 However, the NBSS slope is sensitive enough to reflect the global energy flow and overall
432 efficiency of trophic transfer within the community. NBSS slopes substantially steeper than -1

433 may then suggest that the community TTE is low, which may indicate that single predator-
434 prey interactions or trophic levels in sub-webs may have remained undetected (Lischke et al.
435 2017). Alternatively, a low TTE may indicate the depletion of certain trophic levels by natural
436 or anthropogenic effects, which would cause an interruption in the continuous energy flow
437 from smaller to larger organisms. In turn, NBSS slopes shallower than -1 would indicate
438 TTEs larger than 10%, suggesting that some trophic levels may be subsidized by energy
439 produced outside of the system, for example by terrestrial organic carbon entering aquatic
440 ecosystems, or by highly mobile predators, whose activity ranges are larger than the spatial
441 scale at which the community NBSS has been accumulated (Trebilco et al. 2013).
442 Accordingly, the NBSS slopes can provide information on food web structure and energetic
443 pathways, and can improve the accuracy of TTE estimates.
444 Our approach is based on the combination of empirically derived correlations between the
445 density and size of organisms with the concept of trophic levels in communities which are
446 linked by predation (Trebilco et al. 2013). Therefore, it is an expansion of the energy
447 equivalence rule (Damuth 1981, Nee et al. 1991) and the metabolic-scaling theory (Brown et
448 al. 2004). There are, admittedly, alternative concepts to model community size distributions
449 which do not explicitly consider TTE, but which predict similar NBSS slopes to those
450 calculated in this study. For example, Law et al. (2009) used a stochastic individual-based
451 model for the dynamics of size spectra, based on birth, growth, and death of individuals,
452 resulting in a linear size spectrum with a slope of approximately -1. In another model
453 considering marine zooplankton, the biomass flux from smaller to larger sizes resulted in
454 similar slopes to those calculated here, and emerged from a balance among individual birth,
455 growth, natural death, and predation (Zhou and Huntley 1997). In even more complex
456 community models, many species or groups of animals with similar life histories were linked
457 through feeding interactions, and expended energy on metabolism, growth and reproduction
458 (Andersen and Beyer 2006, Hartvig et al. 2011). In a comprehensive analysis of these kinds of

models, trophic interaction strengths were found to depend only on predator and prey sizes, reaching maximum values at certain PPMR ratios (Rossberg 2012). However, when a high productivity enables all consumers to feed *ad libitum*, the slope of the resulting NBSS again depends on the energy transfer efficiency from smaller to larger species (Rossberg 2012). Therefore, the different approaches to model community size distributions converge in surprisingly similar patterns (Rossberg 2012, Sprules and Barth 2016), because the transfer efficiency between aggregated trophic levels is equivalent to the average individual metabolic net efficiency of the organisms at these trophic levels. Accordingly, the size-related predator-prey interactions and the efficiency of individuals to convert food into biomass are the primary determinants of the empirically documented declines of abundance with increasing organism size in multi-trophic food webs.

In conclusion, community-level indicators such as the NBSS, which are simple to estimate and have a mechanistic ecological basis, may provide insights into the structural and functional properties of ecosystems, which are often difficult to assess directly (Jennings et al. 2008). For example, declining ecosystem stability can be predicted from disrupted slopes of size spectra caused by overfishing or warming, because of the inefficient transfer of energy through the food web and a shift towards faster growth rates and stronger abundance fluctuations of the overall community (Yvon-Durocher et al. 2011, Blanchard et al. 2012). Therefore, the comparison between theoretically predicted and empirically derived community size structures may inform us of the consequences of global warming, species invasions, habitat alterations, and human exploitation on ecosystems processes and services, feeding interactions, and biogeochemical cycles (Blanchard et al. 2017, Brose et al. 2017).

Acknowledgements

We thank Kate Laskowski and Christian Guill for help with the statistical analyses, Jochen Diekmann who analyzed part of the raw data, and two anonymous reviewers whose

comments helped improving the text. The work was funded by grants from the Wissenschaftsgemeinschaft Gottfried Wilhelm Leibniz (WGL) to TM, BL, KA, SB, KS, UG and SH (project TERRALAC) and the Deutsche Forschungsgemeinschaft (DFG) to TM and SB (grant no. Me 1686/7-1).

References

Andersen, K. H. and J. E. Beyer. 2006. Asymptotic size determines species abundance in the marine size spectrum. American Naturalist **168**:54-61.

Best, E. P. H. 1982. The aquatic macrophytes of Lake Vechten - species composition, spatial distribution and production. Hydrobiologia **95**:65-77.

Blanchard, J. L., R. F. Heneghan, J. D. Everett, R. Trebilco, and A. J. Richardson. 2017. From bacteria to whales: using functional size spectra to model marine ecosystems. Trends in Ecology & Evolution **32**:174-186.

Blanchard, J. L., S. Jennings, R. Holmes, J. Harle, G. Merino, J. I. Allen, J. Holt, N. K. Dulvy, and M. Barange. 2012. Potential consequences of climate change for primary production and fish production in large marine ecosystems. Philosophical Transactions of the Royal Society B-Biological Sciences **367**:2979-2989.

Blanchard, J. L., S. Jennings, R. Law, M. D. Castle, P. McCloghrie, M. J. Rochet, and E. Benoit. 2009. How does abundance scale with body size in coupled size-structured food webs? Journal of Animal Ecology **78**:270-280.

Brose, U., J. L. Blanchard, A. Eklof, N. Galiana, M. Hartvig, M. R. Hirt, G. Kalinkat, M. C. Nordstrom, E. J. O'Gorman, B. C. Rall, F. D. Schneider, E. Thebault, and U. Jacob. 2017. Predicting the consequences of species loss using size-structured biodiversity approaches. Biological Reviews **92**:684-697.

509 Brothers, S., Y. Vadeboncoeur, and P. Sibley. 2016. Benthic algae compensate for
510 phytoplankton losses in large aquatic ecosystems. Global Change Biology **22**:3865-3873.
511 Brothers, S. M., S. Hilt, S. Meyer, and J. Köhler. 2013. Plant community structure determines
512 primary productivity in shallow, eutrophic lakes. Freshwater Biology **58**:2264-2276.
513 Brown, J. H. and J. F. Gillooly. 2003. Ecological food webs: High-quality data facilitate
514 theoretical unification. Proceedings of the National Academy of Sciences of the United
515 States of America **100**:1467-1468.
516 Brown, J. H., J. F. Gillooly, A. P. Allen, V. M. Savage, and G. B. West. 2004. Toward a
517 metabolic theory of ecology. Ecology **85**:1771-1789.
518 Buesing, N. and M. O. Gessner. 2003. Incorporation of radiolabeled leucine into protein to
519 estimate bacterial production in plant litter, sediment, epiphytic biofilms, and water
520 samples. Microbial Ecology **45**:291-301.
521 Cyr, H. 1997. Cladoceran- and copepod-dominated zooplankton communities graze at similar
522 rates in low-productivity lakes. Canadian Journal of Fisheries and Aquatic Sciences
523 **55**:414-422.
524 Damuth, J. 1981. Population-density and body size in mammals. Nature **290**:699-700.
525 De Castro, F. and U. Gaedke. 2008. The metabolism of lake plankton does not support the
526 metabolic theory of ecology. Oikos **117**:1218-1226.
527 Gaedke, U. 1992. The size distribution of plankton biomass in a large lake and its seasonal
528 variability. Limnology and Oceanography **37**:1202-1220.
529 Gaedke, U., D. Straile, and C. Pahl-Wostl. 1996. Trophic structure and carbon flow dynamics
530 in the pelagic community of a large lake. Pages 60-71 *in* G. A. Polis and K. O. Winemiller,
531 editors. Food webs. Integration of patterns and dynamics. Chapman & Hall, New York.
532 Hansen, B., P. K. Bjornsen, and P. J. Hansen. 1994. The size ratio between planktonic
533 predators and their prey. Limnology and Oceanography **39**:395-403.

534 Hartvig, M., K. H. Andersen, and J. E. Beyer. 2011. Food web framework for size-structured
535 populations. Journal of Theoretical Biology **272**:113-122.
536 Hilt, S., T. Wanke, K. Scharnweber, M. Brauns, J. Syväranta, S. Brothers, U. Gaedke, J.
537 Köhler, B. Lischke, and T. Mehner. 2015. Contrasting response of two shallow eutrophic
538 cold temperate lakes to a partial winterkill of fish. Hydrobiologia **749**:31-42.
539 Jennings, S. and S. Mackinson. 2003. Abundance-body mass relationships in size-structured
540 food webs. Ecology Letters **6**:971-974.
541 Jennings, S., F. Melin, J. L. Blanchard, R. M. Forster, N. K. Dulvy, and R. W. Wilson. 2008.
542 Global-scale predictions of community and ecosystem properties from simple ecological
543 theory. Proceedings of the Royal Society B-Biological Sciences **275**:1375-1383.
544 Jennings, S., K. J. Warr, and S. Mackinson. 2002. Use of size-based production and stable
545 isotope analyses to predict trophic transfer efficiencies and predator-prey body mass ratios
546 in food webs. Marine Ecology Progress Series **240**:11-20.
547 Kerr, S. R. and L. M. Dickie. 2001. The biomass spectrum. Columbia University Press, New
548 York.
549 Law, R., M. J. Plank, A. James, and J. L. Blanchard. 2009. Size-spectra dynamics from
550 stochastic predation and growth of individuals. Ecology **90**:802-811.
551 Lindeman, R. L. 1942. The trophic-dynamic aspect of ecology. Ecology **23**:399-417.
552 Lischke, B., T. Mehner, S. Hilt, K. Attermeyer, M. Brauns, S. Brothers, H. P. Grossart, J.
553 Köhler, K. Scharnweber, and U. Gaedke. 2017. Benthic carbon is inefficiently transferred
554 in the food webs of two eutrophic shallow lakes. Freshwater Biology **62**:1693-1706.
555 Lischke, B., G. Weithoff, S. A. Wickham, K. Attermeyer, H. P. Grossart, K. Scharnweber, S.
556 Hilt, and U. Gaedke. 2016. Large biomass of small feeders: ciliates may dominate
557 herbivory in eutrophic lakes. Journal of Plankton Research **38**:2-15.
558 Marquet, P. A. 2000. Ecology - Invariants, scaling laws, and ecological complexity. Science
559 **289**:1487-1488.

560 Mehner, T., K. Attermeyer, M. Brauns, S. Brothers, J. Diekmann, U. Gaedke, H. P. Grossart,
561 J. Köhler, B. Lischke, N. Meyer, K. Scharnweber, J. Syväranta, M. J. Vanni, and S. Hilt.
562 2016. Weak response of animal allochthony and production to enhanced supply of
563 terrestrial leaf litter in nutrient-rich lakes. Ecosystems **19**:311-325.
564 Morin, A. and D. Nadon. 1991. Size distribution of epilithic lotic invertebrates and
565 implications for community metabolism. Journal of the North American Benthological
566 Society **10**:300-308.
567 Nee, S., A. F. Read, J. J. D. Greenwood, and P. H. Harvey. 1991. The relationship between
568 abundance and body size in British birds. Nature **351**:312-313.
569 Pauly, D. and V. Christensen. 1995. Primary production required to sustain global fisheries.
570 Nature **374**:255-257.
571 Plante, C. and J. A. Downing. 1989. Production of freshwater invertebrate populations in
572 lakes. Canadian Journal of Fisheries and Aquatic Sciences **46**:1489-1498.
573 Reuman, D. C., C. Mulder, D. Raffaelli, and J. E. Cohen. 2008. Three allometric relations of
574 population density to body mass: theoretical integration and empirical tests in 149 food
575 webs. Ecology Letters **11**:1216-1228.
576 Rogers, A., J. L. Blanchard, and P. J. Mumby. 2014. Vulnerability of coral reef fisheries to a
577 loss of structural complexity. Current Biology **24**:1000-1005.
578 Rossberg, A. G. 2012. A complete analytic theory for structure and dynamics of populations
579 and communities spanning wide ranges in body size. Advances in Ecological Research,
580 Vol 46: Global Change in Multispecies Systems, Pt 1 **46**:427-521.
581 Scharnweber, K., J. Syväranta, S. Hilt, M. Brauns, M. J. Vanni, S. M. Brothers, J. Köhler, J.
582 Knezevic-Jaric, and T. Mehner. 2014. Whole-lake experiments reveal the fate of terrestrial
583 particulate organic carbon in benthic food webs of shallow lakes. Ecology **95**:1496-1505.
584 Sheldon, R. W., W. H. Sutcliff, and A. Prakash. 1972. Size distribution of particles in ocean.
585 Limnology and Oceanography **17**:327-340.

586 Shuter, B. J. and K. K. Ing. 1997. Factors affecting the production of zooplankton in lakes.
587 Canadian Journal of Fisheries and Aquatic Sciences **54**:359-377.
588 Simon, M. and F. Azam. 1989. Protein content and protein synthesis rates of planktonic
589 marine bacteria. Marine Ecology Progress Series **51**:201-213.
590 Sprules, W. G. 2008. Ecological change in Great Lakes communities — a matter of
591 perspective. Canadian Journal of Fisheries and Aquatic Sciences **65**:1-9.
592 Sprules, W. G. and L. E. Barth. 2016. Surfing the biomass size spectrum: some remarks on
593 history, theory, and application. Canadian Journal of Fisheries and Aquatic Sciences
594 **73**:477-495.
595 Stockwell, J. D. and O. E. Johannson. 1997. Temperature-dependent allometric models to
596 estimate zooplankton production in temperate freshwater lakes. Canadian Journal of
597 Fisheries and Aquatic Sciences **54**:2350-2360.
598 Syväranta, J., K. Scharnweber, M. Brauns, S. Hilt, and T. Mehner. 2016. Assessing the utility
599 of hydrogen, carbon and nitrogen stable isotopes in estimating consumer allochthony in
600 two shallow eutrophic lakes. Plos One **11**:ARTN e0155562.
601 Team, R. C. 2016. R: A language and environment for statistical computing. R Foundation for
602 Statistical Computing, Vienna, Austria.
603 Trebilco, R., J. K. Baum, A. K. Salomon, and N. K. Dulvy. 2013. Ecosystem ecology: size-
604 based constraints on the pyramids of life. Trends in Ecology & Evolution **28**:423-431.
605 Vadeboncoeur, Y., M. J. Vander Zanden, and D. M. Lodge. 2002. Putting the lake back
606 together: Reintegrating benthic pathways into lake food web models. Bioscience **52**:44-54.
607 White, E. P., B. J. Enquist, and J. L. Green. 2008. On estimating the exponent of power-law
608 frequency distributions. Ecology **89**:905-912.
609 White, E. P., S. K. M. Ernest, A. J. Kerkhoff, and B. J. Enquist. 2007. Relationships between
610 body size and abundance in ecology. Trends in Ecology and Evolution **22**:323-330.

Yurista, P. M., D. L. Yule, M. Balge, J. D. VanAlstine, J. A. Thompson, A. E. Gamble, T. R. Hrabik, J. R. Kelly, J. D. Stockwell, and M. R. Vinson. 2014. A new look at the Lake Superior biomass size spectrum. Canadian Journal of Fisheries and Aquatic Sciences **71**:1324-1333.

Yvon-Durocher, G., J. M. Montoya, M. Trimmer, and G. Woodward. 2011. Warming alters the size spectrum and shifts the distribution of biomass in freshwater ecosystems. Global Change Biology **17**:1681-1694.

Zhou, M. and M. E. Huntley. 1997. Population dynamics theory of plankton based on biomass spectra. Marine Ecology Progress Series **159**:61-73.

Table 1: Results of a linear mixed effect model to test for differences in biomasses of organisms in the four lake halves. All data pairs of log_2 normalized biomass and log_2 size classes from bacteria to macrozoobenthos of northern and southern halves in both lakes (GS=Gollinsee, SS=Schulzensee) and three seasons (spring, summer, autumn) were included. The degrees of freedom (DF), the F-value and the p-value of the ANOVA are shown.

For non-significant effects, the tendency is shown. Model: log_2(normalized biomass) ~ log_2 size class + lake + season + lake division + lake : log_2 size class + lake division : log_2 size class + (1|lake half) (see methods for model description).

Factor	DF	F-value	p-value	Tendency
Size class	1	7081	< 0.001	
Lake	1	0.4	0.51	GS < SS
Season	2	1.3	0.28	spring < autumn < summer
Lake division	1	0.4	0.55	southern < northern
Lake : size class	1	0.007	0.93	
Lake division : size class	1	0.5	0.50	

633 Table 2: Arithmetic mean group-wise residuals (log_2 normalized biomass) from the linear
634 regression including all data pairs of log_2 normalized biomass and log_2 size class from
635 bacteria to macrozoobenthos for all four lake halves and three seasons combined.

Organismal group	Mean residuals	Number of data points
Pelagic bacteria	-1.65	24
Sediment bacteria	2.57	36
Phytoplankton	0.05	121
Ciliates	0.78	58
Rotifers	-0.67	25
Crustaceans	-1.81	60
Macrozoobenthos	0.24	90

636

637

638

639

Captions of figures:

Figure 1: Normalized biomass size spectra covering aquatic organisms in the size range from bacteria to macrozoobenthos of northern and southern halves of Gollinsee and Schulzensee during spring, summer, and autumn. The slopes and intercepts (calculated by least-squares linear regression), with the respective 95% confidence intervals, and the R^2 of each linear regression (red line) are shown in each subplot. The color coding depicts the organismal group contributing the largest biomass to the respective $\log_2$ size class (pel. bacteria=pelagic bacteria, sed. bacteria=sediment bacteria).

Figure 2: Normalized biomass size spectrum including biomass-size data from bacteria to macrozoobenthos merged from northern (open symbols) and southern (filled symbols) halves of Gollinsee (circles) and Schulzensee (triangles) in spring, summer, and autumn 2011 (season not coded). Group-wise residuals were calculated against the overall linear regression (red line). The slope and intercept as calculated by least-squares linear regression, with the respective 95% confidence intervals, and R^2 of the linear regression (red line) are shown. The color coding depicts the organismal group contributing the largest biomass to the respective $\log_2$ size class (pel. bacteria=pelagic bacteria, sed. bacteria=sediment bacteria).

Figure 3: Comparison of slopes of normalized biomass size spectra (NBSS) as predicted from the empirically estimated trophic transfer efficiency (TTE), and the empirically determined NBSS slopes (± 95% CI) in the northern and southern halves of Lakes Gollinsee and Schulzensee. The open symbol reflects the mean slope (± 95% CI) as predicted from the arithmetic mean TTE from all four lake halves, and the slope and 95% CI from the NBSS merged from all available biomass-size data pairs from all four lake halves. The line of unity (1:1) is given for comparison. A constant predator:prey mass ratio (PPMR) of 10^4 is applied in all cases.

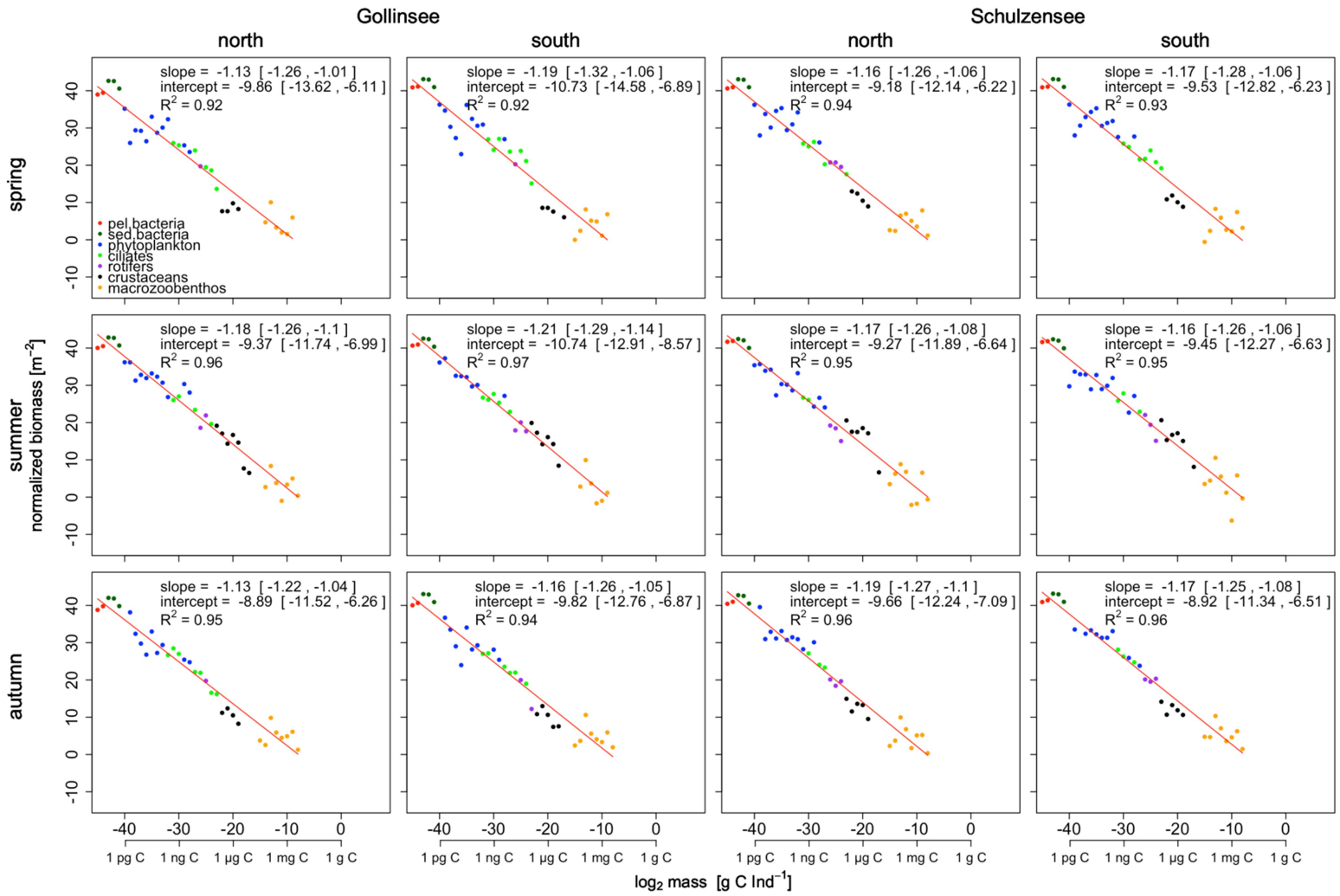
Gollinsee
Schulzensee
north
south
north
south
spring
summer
autumn
normalized biomass [m^{-2}]
slope = -1.13 [-1.26 , -1.01]
intercept = -9.86 [-13.62 , -6.11]
R^2 = 0.92
slope = -1.19 [-1.32 , -1.06]
intercept = -10.73 [-14.58 , -6.89]
R^2 = 0.92
slope = -1.16 [-1.26 , -1.06]
intercept = -9.18 [-12.14 , -6.22]
R^2 = 0.94
slope = -1.17 [-1.28 , -1.06]
intercept = -9.53 [-12.82 , -6.23]
R^2 = 0.93
pel.bacteria
sed.bacteria
phytoplankton
ciliates
rotifers
crustaceans
macrozoobenthos
slope = -1.18 [-1.26 , -1.1]
intercept = -9.37 [-11.74 , -6.99]
R^2 = 0.96
slope = -1.21 [-1.29 , -1.14]
intercept = -10.74 [-12.91 , -8.57]
R^2 = 0.97
slope = -1.17 [-1.26 , -1.08]
intercept = -9.27 [-11.89 , -6.64]
R^2 = 0.95
slope = -1.16 [-1.26 , -1.06]
intercept = -9.45 [-12.27 , -6.63]
R^2 = 0.95
slope = -1.13 [-1.22 , -1.04]
intercept = -8.89 [-11.52 , -6.26]
R^2 = 0.95
slope = -1.16 [-1.26 , -1.05]
intercept = -9.82 [-12.76 , -6.87]
R^2 = 0.94
slope = -1.19 [-1.27 , -1.1]
intercept = -9.66 [-12.24 , -7.09]
R^2 = 0.96
slope = -1.17 [-1.25 , -1.08]
intercept = -8.92 [-11.34 , -6.51]
R^2 = 0.96
-40 -30 -20 -10 0
1 pg C 1 ng C 1 µg C 1 mg C 1 g C
log$_2$ mass [g C Ind^{-1}]

Fig. 1

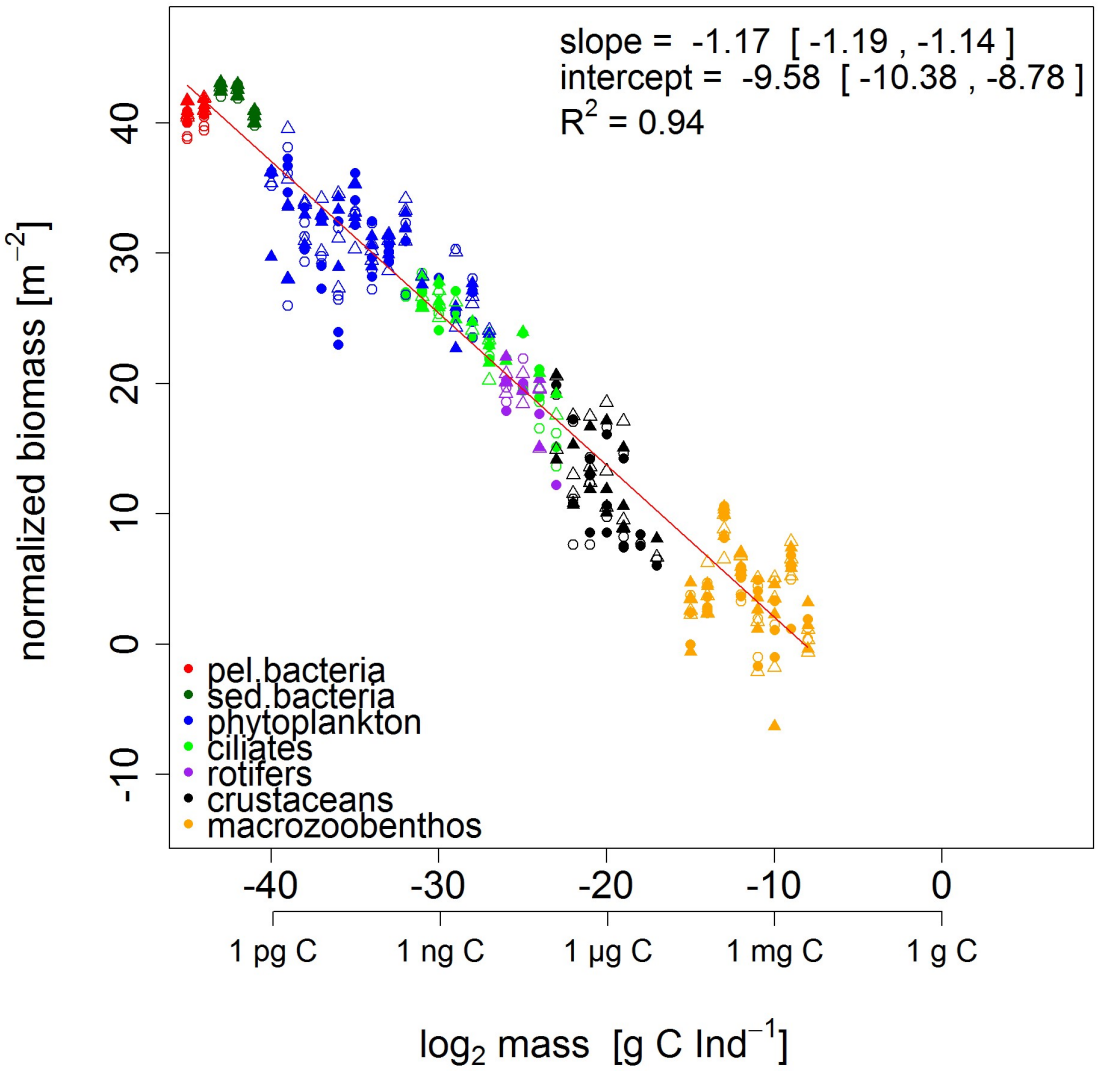
slope = -1.17 [-1.19 , -1.14]
intercept = -9.58 [-10.38 , -8.78]
R2 = 0.94
normalized biomass [m-2]
40
30
20
10
0
-10
pel.bacteria
sed.bacteria
phytoplankton
ciliates
rotifers
crustaceans
macrozoobenthos
-40
-30
-20
-10
0
1 pg C
1 ng C
1 µg C
1 mg C
1 g C
log2 mass [g C Ind-1]

Fig. 2

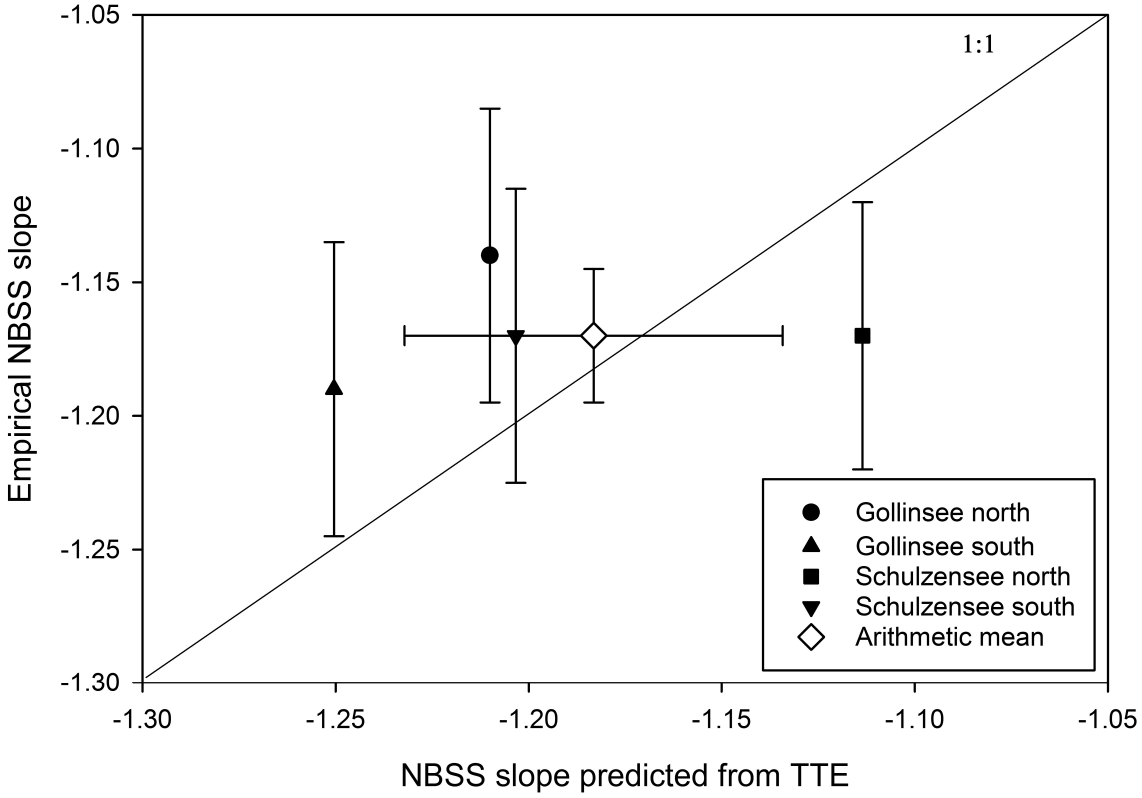
-1.05
-1.10
-1.15
-1.20
-1.25
-1.30
Empirical NBSS slope
1:1
Gollinsee north
Gollinsee south
Schulzensee north
Schulzensee south
Arithmetic mean
-1.30
-1.25
-1.20
-1.15
-1.10
-1.05
NBSS slope predicted from TTE

Fig. 3